



Published in final edited form as:

J Control Release. 2022 February ; 342: 14–25. doi:10.1016/j.jconrel.2021.12.029.

BiTE secretion from *in situ*-programmed myeloid cells results in tumor-retained pharmacology

S. Hao^{a,1}, V.V. Inamdar^{a,1}, E.C. Sigmund^a, F. Zhang^a, S.B. Stephan^a, C. Watson^b, S.J. Weaver^c, U.B. Nielsen^d, M.T. Stephan^{a,e,f,*}

^aClinical Research Division, Fred Hutchinson Cancer Research Center, Seattle, WA 98109, USA

^bComparative Pathology, Fred Hutchinson Cancer Research Center, Seattle, WA 98109, USA

^cExperimental Histopathology, Fred Hutchinson Cancer Research Center, Seattle, WA 98109, USA

^dTidal Therapeutics (A Sanofi Company), 270 Albany St, Cambridge, MA 02139, USA

^eDivision of Medical Oncology, Department of Medicine, University of Washington, Seattle, WA 98195, USA

^fDepartment of Bioengineering and Molecular Engineering & Sciences Institute, University of Washington, Seattle 98195, WA, USA

Abstract

Bispecific T-Cell Engagers (BiTEs) are effective at inducing remission in hematologic cancers, but their use in solid tumors has been challenging due to their extreme potency and on-target, off-tumor toxicities in healthy tissue. Their deployment against solid tumors is further complicated by insufficient drug penetration, a hostile tumor microenvironment, and immune escape. To address these challenges, we developed targeted nanocarriers that can deliver *in vitro*-transcribed mRNA encoding BiTEs to host myeloid cells – a cell type that is actively recruited into the tumor microenvironment. We demonstrate in an immunocompetent mouse model of ovarian cancer, that infusion of these nanoparticles directs BiTE expression to tumor sites, which reshapes the microenvironment from suppressive to permissive and triggers disease regression without systemic toxicity. In contrast, conventional injections of recombinant BiTE protein at doses required to achieve anti-tumor activity, induced systemic inflammatory responses and severe tissue damage in

This is an open access article under the CC BY-NC-ND license (<http://creativecommons.org/licenses/by-nc-nd/4.0/>).

*Corresponding author at: Clinical Research Division, Fred Hutchinson Cancer Research Center, Seattle, WA 98109, USA. mstephan@fredhutch.org (M.T. Stephan).

¹These authors contributed equally to this work.

Credit author statement

Conceptualization: U.B.N. and M.T.S. Data curation: S.H., V.V.I., E.C. S., F.Z., S.B.S., C.W., S.J.W. Formal analysis: S.H., V.V.I., E.C.S., F.Z., S.B.S., C.W., S.J.W., U.B.N., and M.T.S. Funding acquisition: U.B.N., and M.T.S. Investigation: S.H., V.V.I., E.C.S., F.Z., S.B.S., C.W., S.J.W., U.B.N., and M.T.S. Methodology: S.H., V.V.I., E.C.S., F.Z., S.B.S., C.W., S.J.W. Project administration: U.B.N. and M.T.S. Resources: U.B.N. and M.T.S. Software: S.H., V.V.I., E.C.S., and F.Z. Supervision: U.B.N. and M.T.S. Validation: S.H., V.V.I., E.C.S., F.Z. Visualization: U.B.N. and M.T.S. Writing – original draft: M.T.S. Writing – review & editing: M.T.S.

Declaration of Competing Interest

M.T.S. is a consultant of Tidal Therapeutics (a Sanofi company). The remaining authors declare no competing interest.

Appendix A. Supplementary data

Supplementary data to this article can be found online at <https://doi.org/10.1016/j.jconrel.2021.12.029>.

all treated animals. Implemented in the clinic, this *in situ* gene therapy could enable physicians – with a single therapeutic – to safely target tumor antigen that would otherwise not be druggable due to the risks of on-target toxicity and, at the same time, reset the tumor milieu to boost key mediators of antitumor immune responses.

Keywords

In situ gene therapy; Bi-specific T-cell engagers (BiTEs); Nanotechnology

1. Introduction

Redirection of T cells against tumors is an intensely active area of cancer immunotherapy research. One promising approach for T-cell redirection involves the use of recombinant proteins designated bispecific T-cell engagers (BiTEs), which are heterodimers of IgG single-chain fragment variable regions (scFv) with dual specificities for a tumor-associated antigen and CD3 T cells [1]. Binding of multiple BiTE molecules to their respective targets triggers CD3 clustering, T-cell activation and the formation of a pseudoimmunological synapse between the tumor cell and T cell, which induces target cell lysis by apoptosis. Unlike many other T cell-based therapies, BiTE-mediated tumor-cell killing by T cells is independent of HLA expression and can occur in the absence of *ex vivo* prestimulation or costimulatory signals. Despite these unique features, the development of BiTEs to treat cancer patients faces enormous challenges [2]. Currently, only one bispecific antibody construct, Blincyto (blinatumomab), specific for CD3 and CD19, has been approved by the Food and Drug Administration for clinical use in patients, targeting refractory B-cell acute lymphoblastic leukemia [3]. A major hurdle to deploying BiTEs to treat a wider range of malignancies, including solid tumors, is the need to achieve sustained therapeutic drug levels within tumor lesions. BiTEs have to penetrate deeply into the tumor tissues to be able to recruit and activate resident T cells. However, exogenously administered BiTEs are rapidly catabolized and cleared from the circulation, leading to a short serum half-life [4]. To counter-balance rapid elimination, BiTE proteins must be given as a continuous infusion over weeks, thereby exposing patients to high systemic doses, which can be accompanied by severe toxicity [5]. Thus, a second critical barrier which has prevented most BiTE antibody formats from reaching Phase 3 clinical trials is on-target, off-tumor toxicity. By and large, the target molecules of these antibody derivatives are differentiation antigens present not only on malignant cells, but also on their non-transformed counterparts, and engagement of the latter often generates serious, if not lethal, adverse events.

One prominent example is Solitomab, an anti-EpCAM (Epithelial Cell Adhesion Molecule) × CD3 bispecific antibody construct developed by Amgen [6]. EpCAM is an attractive therapeutic target because it is highly expressed on various human carcinomas, in particular on difficult-to-treat chemotherapy-resistant tumor cells as well as on cancer stem cells [7]. Like most cancer immunotherapy targets, EpCAM can also be present at lower levels on normal tissues; it is predominantly expressed in the basolateral and intercellular surfaces of healthy epithelia [8]. Consequently, severe autoimmune adverse effects were observed in a Phase 1 study of Solitomab in patients with refractory solid tumors, which impeded dose

escalation to therapeutic levels [9]. Similar dose-limiting toxicities were observed in clinical studies of BiTEs targeting other solid tumor targets, such as HER2, PSMA or CEA, and successful BiTE therapy of solid tumors has not been reported so far [10–12].

To achieve persistent and effective concentrations of BiTE antibodies in the tumor microenvironment and reduce systemic exposure, chimeric antigen receptor (CAR) T cells have been genetically modified to secrete BiTE antibodies [13]. Post-infusion, some of these T cells migrate to tumor sites and simultaneously act as antibody factories and effectors. However, adoptive T-cell therapy requires isolation of lymphocytes and genetically modifying them with complex laboratory procedures that are not available to most patients. Several groups have developed oncolytic viruses as readily available agents to achieve tumor-targeted expression of BiTEs *in situ* [14]. However, this approach is limited to direct intratumor delivery and cannot be employed in multifocal or inaccessible tumors. Furthermore, oncolytic viruses induce a strong innate immune response which, together with preexisting circulating antibodies, triggers their clearance [15].

In vitro-transcribed (IVT) mRNA has emerged as a disruptive new drug class which can be used to encode therapeutically relevant proteins that are translated within target cells *in vivo* [16,17]. Synthetic mRNA molecules can be quickly designed, manipulated and mass-produced relatively cost-effectively [18]. Over the past decades, scientists have learned how to optimize mRNA pharmacologically and immunologically to make it more drug-like for clinical applications [19–22]. Here, we developed an injectable nanoreagent that carries synthetic mRNA to program *in situ* circulating myeloid cells to secrete functionally active BiTE antibodies (Fig. 1). Myeloid cells are ideal vehicles for the endogenous secretion of T-cell-redirecting bispecific antibodies because the cells easily reach tumors, are attracted by secreted chemokines, and infiltrate hypoxic areas [23]. Using the fully immunocompetent ID8-VEGF model for stage 3 ovarian carcinoma, we demonstrate that, when administered periodically, polymeric nanoparticles encoding a murine version of the EpCAM × CD3 bispecific antibody can achieve high gene transfer into circulating myeloid cells, which subsequently secrete BiTEs and effectively concentrate this drug at tumor sites. This action substantially reduced tumor progression and, in most animals, even cleared the disease without detectable systemic toxicity. In contrast, conventional infusions of recombinant EpCAM × CD3 BiTE protein had no effect in this test system, unless administered at a high dose, which then triggered fatal adverse events in all animals. Phenotypic and gene expression studies revealed that, in addition to activating T cells against tumor, endogenous secretion of BiTE constructs from myeloid cells reprogrammed these cells toward an anti-tumor (M1-like) phenotype. This reversed the immunosuppressive state of the tumor microenvironment and enabled optimal T effector cell infiltration and antitumor function.

BiTEs are one of the most promising areas in immuno-oncology research owing to their potential to draw active T cells to cancer cells, but without the complex manufacturing processes of CAR T cells; however, like CAR T cells, their move from hematological malignancies to solid tumors has been slow. We demonstrate that a BiTE-encoding mRNA nanodrug enables preferential permeation of the BiTE into tumor tissue, making the therapy more efficacious and safer compared to conventional infusions of BiTE antibodies. Given

their ease of manufacturing, distribution and administration, these nanocarriers, and the associated platforms, could greatly expand the therapeutic index of T-cell engagers.

2. Materials and methods

2.1. Cell lines

The murine ovarian cancer cell line ID8, a gift from Dr. Katherine Roby (University of Kansas Medical Center, Kansas City, KS) [24], was cultured in DMEM supplemented with 4% fetal bovine serum (FBS) and 5 $\mu\text{g}/\text{ml}$ insulin, 5 $\mu\text{g}/\text{ml}$ transferrin, and 5 ng/ml sodium selenite (all Sigma-Aldrich). To generate the more aggressive Vascular Endothelial Growth Factor (VEGF)-expressing strain, we transfected ID8 tumor cells with the pUNO1 plasmid (InvivoGen) encoding murine VEGF and the blasticidin-resistance gene. To obtain stable transfectants, tumor cells were cultured in complete medium containing 10 $\mu\text{g}/\text{ml}$ blasticidin (InvivoGen) for three weeks. To generate EpCAM-expressing ovarian tumor cells, ID8-VEGF cells were stably transduced with EpCAM-encoding lentiviral vector. EpCAM+ tumor cells were isolated using fluorescence-activated cell sorting. RAW246.7 cells were purchased from ATCC and cultured in DMEM supplemented 10% FBS.

2.2. mRNA

Codon-optimized mRNAs for eGFP, mCherry and EpCAM \times CD3 BiTE were obtained from TriLink Biotechnologies. mRNA transcript was modified with full substitution of N1-Methyl-Pseudo-U Capped using CleanCap AG polyadenylated (120A), DNase and phosphatase treatment and purified by silica membrane.

2.3. PbAE synthesis

1,4-Butanediol diacrylate was combined with 4-amino-1-butanol in a 1:1 M ratio of diacrylate to amine monomers. Acrylate-terminated poly (4-amino-1-butanol-co-1,4-butanediol diacrylate) was formed by heating the mixture to 90°C with stirring for 24h. 2.3g of this polymer was dissolved in 2 ml tetrahydrofuran (THF). To form the piperazine-capped 447 polymer, 786mg of 1-(3-aminopropyl) – 4-methylpiperazine in 13mL THF was added to the polymer/THF solution and stirred at room temperature (RT) for 2h. The capped polymer was precipitated with 5 volumes of diethyl ether, washed with 2 volumes of fresh ether, and dried under vacuum for 1 day. Neat polymer was dissolved in dimethyl sulfoxide (DMSO) to a concentration of 100mg/mL and stored at -20°C.

2.4. PGA conjugation to Di-mannose

α -D-mannopyranosyl-(1 \rightarrow 2)- α -D-mannopyranose (Di-mannose, Omicron Biochemicals Inc.) was modified into glycosylamine before being conjugated to polyglutamic acid (PGA). First, the Di-mannose (157 mg) was dissolved in 10.5 ml of saturated aqueous ammonium carbonate, then stirred at RT for 24 h. On the second day, more solid ammonium carbonate was added until the Di-mannose precipitated from the reaction solution. The mixture was stirred until completion, as measured by TLC, followed by lyophilization to remove the excess ammonium carbonate. Complete removal of volatile salt was accomplished by re-dissolving the solid in methanol. These procedures created an amine on the anomeric carbon for future conjugation with PGA.

To conjugate aminated Di-mannose to PGA, the substrate was dissolved in water to 30 mg/mL, then sonicated for 10 min. Ethyl-N'-(3-dimethylaminopropyl) carbodiimide•HCl in water (4 mg/ml, 30 equiv.) was added with mixing at RT for 4 min. N-hydroxysulfosuccinimide in water (30 mg/ml, 35 equiv.) was incubated with the PGA/EDC solution for 1 min. Aminated Di-mannose in phosphate-buffered saline (PBS) was combined with the resulting activated PGA in a 44:1 M ratio and mixed at RT for 6 h. Excess reagents were removed by dialysis against water for 24 h.

2.5. Nanoparticle preparation

IVT mRNA was diluted to 100 µg/ml in 25 mM sodium acetate (NaOAc) buffer (pH 5.2). Poly(β-amino esters)-447 (PbAE-447) polymer in DMSO (prepared as described above) was diluted from 100 µg/µl to 6 µg/µL, also in NaOAc buffer. To form the nanoparticles, PbAE-447 polymers were added to the mRNA at a ratio of 60:1 (w:w) and vortexed immediately for 15 s at a medium speed, then the mixture was incubated at RT for 5 min to allow the formation of PbAE-mRNA polyplexes. In the next step, 100 µg/mL PGA/Di-mannose in NaOAc buffer was added to the polyplexes solution, vortexed for 15 s at medium speed, and incubated for 5 min at RT. In this process, PGA/Di-mannose coats the surfaces of the PbAE-mRNA polyplexes to form the final nanoparticles. For long-term storage, D-sucrose (60 mg/mL) was added to the nanoparticle solutions as a cryoprotectant. The nanoparticles were snap-frozen in dry ice, then lyophilized. The dried nanoparticles were stored at -20 °C or -80 °C until use. For *in vivo* experiments, lyophilized nanoparticles were re-suspended in water at a 1:20 (w:v) ratio.

2.6. Characterization of nanoparticle (NP) size distribution and ζ-potential

The physiochemical properties of NPs (including hydrodynamic radius, polydispersity, ζ-potential, and stability) were characterized using a Zetapals instrument (Brookhaven Instrument Corporation) at 25 °C. To measure the hydrodynamic radius and polydispersity based on dynamic light scattering, NPs were diluted 5-fold into 25 mM NaOAc (pH 5.2). To measure the ζ-potential, NPs were diluted 10-fold in 10 mM PBS (pH 7.0). To assess the stability of NPs, freshly prepared particles were diluted in 10 mM PBS buffer (pH 7.4). The hydrodynamic radius and polydispersity of NPs were measured every 10 min for 5 h, and their sizes and particle concentrations were derived from Particle Tracking Analysis using a Nanosite 300 instrument (Malvern). Freshly made NPs (25 µL containing 0.83 µg of mRNA) were deposited on glow discharge-treated 200 mesh carbon/Formvar-coated copper grids. After 30 s, the grids were treated sequentially with 50% Karnovsky's fixative, 0.1 M cacodylate buffer, dH₂O, then 1% (w/v) uranyl acetate. Samples were imaged with a JEOL JEM-1400 transmission electron microscope operating at 120 kV (JEOL USA).

2.7. Expression of recombinant BiTE protein

EpCAM × CD3 BiTE protein was expressed and purified by ATUM Biosciences (Newark, California, USA). The protein sequence is shown in Supplementary Fig. 1.

2.8. BiTE quantification by ELISA

EpCAM × CD3 BiTE concentrations were quantified by c-tag ELISA developed in house. Briefly, 96-well streptavidin-coated plates (Thermo Fisher) were incubated with biotinylated anti-c-tag conjugates (100 µl/well at 10 µg/ml; Thermo Fisher) diluted in PBS overnight at 4 °C. After blocking the plates with 20% newborn calf serum in PBS, serum samples and protein standards were added to the wells for incubation. Recombinant mouse EpCAM Fc chimera (Bio-Techne) was added to the wells at 5 µg/ml. After extensive washing, HRP Rat anti-Mouse IgG2a antibody (1:7500; Thermo Fisher) was added to the wells. After incubation with TMB substrates, the reaction was stopped, and ODs were determined at 450 nm with wavelength correction at 630 nm using a Synergy H4 Microplate Reader (BioTek). Samples were assayed in duplicate. For *in vitro* studies, samples were normalized to average values obtained from wells containing cells transfected by control nanoparticles.

2.9. Mice and in vivo tumor models

All mice used in our experiments were obtained from Jackson Laboratory. All mice were handled in accordance with protocols approved by the Center's *Institutional Animal Care and Use Committee*. To model ovarian tumors, 5×10^6 EpCAM-expressing ID8 cells were injected intraperitoneally (i.p.) into 4- to 6-week-old female albino B6 (C57BL/6 J-Tyr < c-2 J>) mice or female tdTomato (C57BL/6 J-*Gt(ROSA)26Sor^{tm14(CAG-tdTomato)Hze}*) mice and allowed to establish for 1 week. Mice were treated according to the timelines and dosing regimens shown in the figures.

2.10. Cytokine analysis

Cytokine levels were measured using a Luminex 200 system (Luminex) at the FHCRC Immune Monitoring Shared Resource core facility. Serum was collected from the treated animals at the end of the *in vivo* toxicity study for measurement of IFN- γ , TNF- α , IL-2 and IL-6.

2.11. Western blotting

Protein samples were separated by SDS-PAGE and transferred onto PVDF membranes using a Mini-PROTEAN Tetra System (Bio-Rad Laboratories). Membranes were incubated in blocking buffer on a shaker for 30 min and washed three times in TBST. Membranes were probed with biotinylated anti-c-tag conjugates (1:2000; Thermo Fisher) overnight at 4 °C followed by an incubation with IRDye 680RD Streptavidin (1:3000; LI-COR Biosciences) for 2 h at RT, avoiding light. Membranes were imaged using an Odyssey CLx imager (LI-COR Biosciences) and analyzed using Image Studio software.

2.12. In vivo bioluminescence imaging

D-Luciferin (Xenogen) in PBS (15 mg/mL) was used as a substrate for firefly luciferase imaging. Bioluminescence images were collected with a Xenogen IVIS Spectrum Imaging System (Xenogen). Mice were anesthetized with 2% isoflurane (Forane, Baxter Healthcare) before and during imaging. For ID8-VEGF-EpCAM ovarian tumors, each mouse was injected i.p. with 300 µg of D-Luciferin, and images were collected 10 min later. Acquisition

times ranged from 10 s to 5 min. Data were analyzed using IVIS Living Image 4.7.2 software.

2.13. Flow cytometry and cell sorting

Cells were analyzed by flow cytometry using the antibody probes listed in Supplementary Table 1. Data were collected using a BD LSRFortessa analyzer running FACSDIVA software (Beckton Dickinson). CD11b + mCherry+ monocytes (Fig. 8) were sorted using a BD FACS ARIA II. All collected data were analyzed using FlowJo 10.0 software.

2.14. RNA isolation and purification

To harvest RNAs, collected cells and tissues were homogenized in TRIzol reagent (Ambion) followed by freezing and then thawing the samples. Total RNA was isolated and purified by chloroform extraction, followed by isopropanol precipitation and ethanol wash for two times. RNA pellets were resuspended in water. Sample RNA was quantified using a NanoDrop Microvolume Spectrophotometer (Thermo Fisher).

2.15. Macrophage signature gene analysis using NanoString technology

Gene expression profiles of sorted peritoneal macrophages were assessed using nCounter Mouse Myeloid Innate Immunity v2 Panel (NanoString Technologies), which characterizes 734 immunology-related mouse genes in 19 signaling pathways representing seven different myeloid cell types. The RNA samples were processed and tested using an nCounter Analysis System (NanoString Technologies). The quality of the raw data was examined by the Quality Control function in nSolver Analysis Software 4.0 (NanoString Technologies). The gene expression levels were normalized to the geometric means of positive controls and 20 housekeeping genes. Pathway analysis was performed on selected gene sets from each sample's gene expression profile.

2.16. Histology

Immunofluorescence, immunohistochemistry (IHC), and hematoxylin and eosin (H&E) analyses were performed on mouse intestinal mesentery tissue. For all histopathology analyses, tissues were fixed in 4% neutral buffered formalin for at least 48 h before further processing. Four-micron sections were cut from each paraffin-embedded tissue and stained with the Leica Bond Rx (Leica Biosystems). For IHC DAB staining, slides were pretreated with Leica Bond Epitope Retrieval Solution for 20 min. Endogenous peroxidase was blocked with Leica peroxide block for 5 min. A TCT protein block was applied for 10 min (0.05 M Tris, 0.15 M NaCl, 0.25% Casein, 0.1% Tween 20, 10% mouse serum, pH 7.6). Primary antibody was applied to the slides for 60 min. The antibody was then detected using a specific polymer and staining was visualized with BOND Polymer Refine Detection DAB (Leica Biosystems); a hematoxylin counterstain was also used (Leica Biosystems). Primary antibodies applied in the immunofluorescence and IHC DAB analysis are listed in Supplementary Table 2. A Perkin Elmer Vectra 3.0 Automated Imaging Platform was used to acquire images of the intestinal mesentery slides. The images are presented at 1.5×, 5×, 10× or 20× magnification, with scale bars indicated. To quantify immune cell populations in the tumor tissues, the images were analyzed using HALO Image

Analysis Modules. The HighPlex FL v3.2.1 function was applied to quantify %F4/80⁺ cells, %Ly-6B.2⁺ cells, %CD8⁺ cells and %CD4⁺ cells among all the cells in the tumor region. To assess nanoparticle-transfected F4/80⁺ macrophages in the tumor lesions, the percentage of tdTomato⁺ cells among F4/80⁺ cells was quantified. For each sample group, five slides prepared from intestinal mesentery tissue of three animals were analyzed.

2.17. Statistical analyses and data presentation

For continuous variables, results are presented as mean \pm SD. The statistical significance of observed differences between any two groups was analyzed by unpaired, two tailed Student's *t*-test assuming unequal variance. The *P* values are presented on the figures or in the figure legends. Comparison of survival curves was made using the Log-rank (Mantel-Cox) test. All the statistical analyses were performed using GraphPad Prism version 8.0 (GraphPad Software).

2.18. Study approval

The care and use of mice in this study were approved by the Institutional Animal Care & Use Committee (IACUC) at the Fred Hutchinson Cancer Research Center and complied with all relevant ethical regulations for animal testing and research (Assurance #A3226-01, IACUC Protocol Number 50782).

3. Results

3.1. BiTEs secreted by nanoparticle-transfected myeloid cells are functional

We developed a targeted mRNA delivery system that can introduce robust gene expression in the targeted cells by taking advantage of electrostatic interactions between cationic poly(β -amino ester) (PbAE) polymers and anionic mRNA (Fig. 2a). To improve the stability and translation of the mRNA encapsulated in the nanocarriers, we used synthetic versions of the message that incorporate the modified ribonucleotides pseudouridine and 5-methylcytidine, and that are capped with ARCA (Anti-Reverse Cap Analog) [25].

We chose a BiTE antibody bispecific for murine EpCAM and CD3, which consists of

the rat-anti-mouse EpCAM-specific G8.8 scFv fused to the anti-murine CD3 2C11 scFv sequence (Supplementary Fig. 1). A c-tag was added at the c-terminus of the BiTE for easy quantification and detection using ELISA. EpCAM is widely expressed on most human adenocarcinoma, several squamous cell carcinoma and cancer stem cells, but also on various normal epithelial tissues [8]; thus, it is representative of the antigens expressed on malignant and non-malignant cells against which bispecific antibodies are in clinical development. To target the nanoparticles to myeloid cells as well as further stabilize the mRNA-PbAE complexes they contain, we engineered Di-mannose moieties onto their surface using polyglutamic acid (PGA) as a linker. The nanoparticles were manufactured by using a simple two-step, charge-driven self-assembly process. First, the synthetic mRNA was complexed with a positively-charged PbAE polymer, which condenses the mRNA into nano-sized complexes. This step was followed by the addition of PGA functionalized with Di-mannose, which shields the positive charge of the PbAE-mRNA particles and confers

macrophage-targeting. The resulting mRNA nanocarriers had a size of $156.4 \pm \text{SE}/7.2$ nm, a polydispersity of 0.281, and a negative surface charge ($-38.5 \pm \text{SE}/0.2$ mV ζ -potential). Following a single nanoparticle application, we routinely transfected 88.1% ($\pm \text{SE}/2.7\%$; $n = 6$) of myeloid cells without reducing their viability (Fig. 2b).

We next confirmed the integrity of the EpCAM \times CD3 BiTE protein obtained from the supernatants of myeloid cells transfected with mRNA nanoparticles, and measured secretion levels over time. Western blotting detected a protein at the predicted molecular weight of ~ 55 kDa (Fig. 2c). Serial ELISA measurements revealed a peak BiTE secretion averaging 428.87 ± 62.71 ng protein per one million transfected cells on day 1 after nanoparticle exposure. As expected, BiTE secretion was transient, and was reduced to 25.06 ± 17.31 ng protein per one million transfected cells after 3 days in culture (Fig. 2d). To verify that the EpCAM \times CD3 BiTE antibodies engage T cells, redirect T-cell-mediated cytotoxicity, and ultimately kill EpCAM-positive target cells, we used a luciferase-based T-cell-dependent cellular cytotoxicity assay. Mouse tumor cells expressing firefly luciferase and various levels of EpCAM antigen were co-cultured with non-activated mouse T cells and with titrated EpCAM \times CD3 BiTE protein (Fig. 2e). Using *in vitro* bioluminescence as the readout, we observed dose-dependent redirected lysis of murine EpCAM-expressing ID8 ovarian cancer cells only when T cells and BiTEs were combined in the cell culture assay (Fig. 2f, g). T-cell activation (Fig. 2h, i) and secretion of the pro-inflammatory cytokine IFN γ (Fig. 2j) were only evident when T cells encountered EpCAM-positive ID8 tumor cells. These results demonstrate that the EpCAM \times CD3 BiTE construct is fully functional and that it mediates cytotoxicity and T-cell activation only in the presence of tumor-associated antigen-expressing cells.

3.2. Therapeutic effects of nanoparticle-delivered EpCAM \times CD3 BiTE genes for disseminated ovarian cancer

To evaluate this treatment approach in a clinically relevant *in vivo* test system, we used a model that recapitulates late-stage, unresectable ovarian tumors in C57BL/6 mice; these animals are injected with ID8-EpCAM ovarian cancer cells tagged with luciferase to enable serial bioluminescent imaging of tumor growth [26,27]. The tumors were allowed to establish for seven days. By this stage, the mice have developed nodules throughout the peritoneal wall and in the intestinal mesentery. We tested both intraperitoneal and intravenous drug administration routes. Intraperitoneal chemotherapy, given in cycles over 6–9 weeks, is now the standard of care for ovarian cancer patients, so clinical protocols are established on how to best place, maintain and eventually remove the catheter [28]. The intraperitoneal catheter is usually left in patients for 9 weeks and weekly nanoparticle dosing would be acceptable. As a first step, we confirmed that Di-mannose functionalized mRNA nanoparticles preferentially transfect macrophages and monocytes *in situ* (Supplementary Fig. 2). To investigate the therapeutic benefit of this technology, animals were divided into groups that received phosphate-buffered saline (PBS) (control), recombinant EpCAM \times CD3 BiTE protein at escalating doses, or EpCAM \times CD3 BiTE mRNA nanoparticle treatment. We used bioluminescence imaging to serially quantify tumor growth and monitored overall survival. We observed that in the BiTE mRNA nanoparticle-treated group, the disease regressed and was eventually cleared in 60% (i.p. route; Fig. 3a–c) and 50% (i.v. route; Fig.

3d–f) of animals. In contrast, infusions of recombinant BiTE antibody, even at maximum tolerated doses (10 µg for i.p. and 2 µg for i.v. administration), yielded a modest 3-day and 16.5-day survival advantage, respectively, compared with untreated control animals. Higher doses triggered severe autoimmune toxicities that led to the death of animals within one week (Fig. 3b, e).

3.3. BiTE secretion from in situ-programmed myeloid cells is not associated with systemic toxicities that accompany infusion of recombinant BiTE protein

To understand how infusion of recombinant EpCAM × CD3 BiTE protein can cause lethality, we first measured EpCAM expression in normal *versus* malignant tissues in mice bearing established ID8-EPCAM ovarian tumor. Confocal microscopy analysis revealed strong EpCAM expression in the intestine, pancreas, kidney, fallopian tube, and the cystic duct (Fig. 4). In direct comparison, ovarian tumor lesions expressed more moderate and heterogeneous levels of EpCAM, which recapitulates tumor antigen heterogeneity in human disease [7].

Guided by this antigen expression profile, we next conducted a comprehensive toxicity assessment. Mice were injected intravenously with EpCAM × CD3 BiTE protein or mRNA nanoparticles encoding this BiTE protein, according to the experimental timelines shown in Fig. 5a. These treatment schedules were based on the dosing which achieved the greatest therapeutic benefits in our tumor challenge experiments (Fig. 3d–f). Mice were euthanized on day 11, blood was collected by retro-orbital bleed for serum chemistry, and a complete gross necropsy was performed. The following tissues were evaluated by a board-certified staff pathologist: liver, pancreas, spleen, and kidney. Serum chemistry of animals treated with recombinant EpCAM × CD3 BiTE protein revealed a marked elevation in the liver enzymes ALT (mean 3.6-fold increase) and AST (mean 1.6-fold increase), an increase in cholesterol (mean 2.7-fold), and a mean 2.4-fold decrease in glucose (Fig. 5b). These changes can indicate compromised liver function and cholestasis, although microscopic evidence of the latter was not seen. The liver elevations are likely a result of pronounced microscopic changes, including hepatocyte necrosis, mixed cell inflammation of the portal triads/central veins, and fatty vacuolar degeneration (Fig. 5c). Posthepatic cholestasis can be caused by pancreatic necrosis and inflammation, also seen in this treatment group (Fig. 5c). A decrease in glucose could be an indication of septicemia [29]; however, there was no gross or histopathological evidence of this. In sharp contrast, in mice treated with BiTE-encoding mRNA nanoparticles, serum chemistry values (including liver- and kidney function) were comparable to those of controls (Fig. 5b). The few histological lesions noted, inflammatory infiltrates in the liver and pancreas, were minimal to mild (Fig. 5c). In parallel experiments we also serially monitored serum levels of the inflammatory cytokines interleukin-2 (IL-2), interferon gamma (IFN-γ), tumor necrosis factor alpha (TNF-α), and interleukin-6 (IL-6). Cytokine release syndrome due to massive T-cell stimulation is a potentially life-threatening *toxicity triggered by* T cell-engaging immunotherapeutics [30]. Following a single infusion of 10 µg EpCAM × CD3 BiTE protein, we measured a rapid increase in serum levels of IL-2 that peaked at a mean of 7979 pg/ml (± 872 pg/mL) after 2 h (Fig. 5d). TNF-α and IL-6 had similar kinetic profiles to IL-2, reaching maximum serum levels (mean 667 pg/mL ± 843 pg/ml and mean 3430 pg/ml ± 1212 pg/ml, respectively) 2 h post BiTE protein

infusion. IFN- γ concentration showed a more gradual increase, reaching a maximum (mean 5068 ± 1512 pg/ml) after 8 h (Fig. 5d). No significant increases in IL-2 and TNF- α were measured in mice treated with BiTE-encoding mRNA nanoparticles. IFN- γ concentration was modestly increased (7.8-fold lower peak levels compared to peak serum levels in BiTE protein-treated mice). IL-6 increased to a mean of 2731 pg/ml (± 999 pg/ml) after 2 h, which was similar to the peak we measured in BiTE protein-infused animals (Fig. 5d). Notably, when measuring IL-2, TNF and IFN- γ cytokine levels directly in ID8-EpCAM ovarian tumor lesions following therapy, we noticed robustly elevated levels following EpCAM \times CD3 BiTE mRNA nanoparticle treatment compared to conventional BiTE protein infusion (Supplementary Fig. 3).

Overall, our data establish that the safety profile of BiTEs can be significantly improved through the use of nanoreagents that carry synthetic mRNA to *in situ* program circulating myeloid cells to secrete functionally active BiTE antibodies.

3.4. Secretion of T-cell engagers from *in situ*-programmed myeloid cells results in limited systemic exposure and tumor-retained pharmacology

To determine whether *in situ* expression of bispecific antibodies from nanoparticle-transfected myeloid cells reduces the high systemic drug exposure observed following infusion of BiTE protein, we conducted an *in vivo* mouse pharmacokinetics (PK) study. Following a single i.v. or i.p. dose into ovarian tumor-bearing mice, BiTE levels in the peripheral blood and the peritoneum were measured by ELISA. We observed maximum BiTE concentrations in the serum and peritoneum immediately following i.v. or i.p. injection of recombinant BiTE protein (Fig. 6a–b). BiTE protein levels then dropped sharply and were undetectable after 12 h. In direct comparison, *in situ* expression of BiTEs from nanoparticle-transfected myeloid cells resulted in an average 194-fold lower maximum systemic BiTE exposure following i.v. nanoparticle administration (peak levels after 24 h; Fig. 6a), and an average 9.2-fold lower maximum intraperitoneal BiTE exposure following direct i.p. administration (peak levels after 12 h; Fig. 6b). Instead of the initial brief protein pulse observed following infusion of recombinant protein, we detected more-sustained, low-level BiTE concentrations after administration of BiTE-encoding mRNA nanoparticles (Fig. 6a, b). Of note, systemic infusion of recombinant protein quickly increased BiTE concentrations in the peritoneal fluid (Fig. 6c). Conversely, i.p.-administered BiTE protein was swiftly absorbed into the circulation (Fig. 6d). We could not entirely prevent this unwanted drug leakage by switching to mRNA, but substantially reduced the maximum systemic BiTE exposure by an average 10.9-fold (peak levels after 24 h; Fig. 6d).

We next shifted our focus to the tumor lesions and examined whether the use of macrophage-targeted mRNA nanoparticles can substantially improve BiTE tumor penetration. As a first step, we quantified trafficking of *in situ*-transfected myeloid cells to tumor sites. To sensitively identify mRNA-transfected cell populations *in vivo*, we employed the Ai14 reporter mouse [31]. In this genetically modified model, all cells contain a loxP-flanked STOP cassette preventing transcription of a CAG promoter-driven tdTomato protein. Only cells that are successfully transfected with mRNA encoding Cre recombinase (Cre) are able to excise the loxP-flanked STOP cassette, resulting in

permanent tdTomato transcription and subsequent strong, amplified tdTomato expression. Using immunohistochemical staining to visualize and quantify tumor infiltration of *in situ*-transfected myeloid cells, we found an average 3.4% ($\pm 1.2\%$) of myeloid cells in tumor lesions to be tdTomato-positive (Fig. 7a, top panel). Overlay immunofluorescence staining confirmed specific co-localization of tdTomato and the macrophage marker F4/80 (Fig. 7a, bottom panel). To study in more detail how BiTE secretion from tumor-associated macrophages affects the tumor immune cell composition, we quantified lymphocyte and neutrophil infiltration into tumors using automated image analysis. We found that treatment with EpCAM \times CD3 BiTE mRNA nanoparticles increased T-cell infiltration into tumors by an average 5.2-fold (CD8) and 2.5-fold (CD4; Fig. 7b, c). Also, the densities of myeloid cells and neutrophils increased by 1.9-fold and 5.6-fold, respectively (Fig. 7d, e).

3.5. Endogenous secretion of BiTEs from macrophages repolarizes them from suppressive to permissive

Guided by this histologic analysis, we hypothesized that secretion of BiTE constructs and subsequent recruitment and activation of T cells would reverse the M2-like immunosuppressive state of tumor-homing macrophages and reprogram them to an M1-like phenotype that induces anti-tumor immunity and promotes tumor regression. To study how EpCAM \times CD3 BiTE-encoding nanoparticles affect the fate of *in situ*-transfected myeloid cells, we performed a NanoString gene expression analysis on CD11b + cells isolated from ovarian tumors of nanoparticle-treated vs. untreated mice (Fig. 8a). To ensure that only successfully transfected cells were analyzed, we co-delivered mRNA encoding BiTE and a FACSable reporter (mCherry). We found that a wide range of signature M1 macrophage genes, such as tumor necrosis factor (TNF), MyD88, Intercellular adhesion molecule-1 (ICAM-1), or Interferon regulatory factor 5 (IRF5), were upregulated as a result of BiTE mRNA nanoparticle transfection. Conversely, signature M2 macrophage genes, such as Arginase 1 (Arg1), Resistin-like alpha (Retnla), Interleukin-10 (IL-10), or C-C Motif Chemokine Ligand 17 and 24 (CCL17, CCL24), were downregulated, compared to untreated controls (Fig. 8b–d). Notably, we also measured elevated expression of multiple genes involved in T-cell recruitment, in particular Chemokine (C-X-C) ligand 9 and 10 (Cxcl9, Cxcl10), or Chemokine (C-C motif) receptor 2 and 7 (Ccl2, Ccl7; Fig. 8e), which correlates with the robust T-cell infiltration into ovarian tumors we observed following EpCAM \times CD3 BiTE mRNA therapy (Fig. 7b, c). Flow cytometry confirmed downregulation of the M2 macrophage marker CD206 in tumor-infiltrating macrophages following injections of BiTE-encoding mRNA nanoparticles (Supplementary Fig. 4). Taken together, these data establish that endogenous nanoparticle-mediated expression of BiTE constructs skews suppressive macrophages toward a proinflammatory phenotype and renders the tumor microenvironment permissive for infiltration and expansion of T lymphocytes.

4. Discussion

This study demonstrates that therapeutic efficacy of BiTEs against solid tumors can be achieved by means of synthetic mRNA nanoparticles that program BiTE-secreting capabilities into myeloid cells *in vivo*. We describe the production of bispecific antibodies in tumor lesions leading to local T-cell infiltration and remodeling of the tumor milieu

without causing systemic toxicities. The *in situ* gene therapy we developed avoids many of the drawbacks associated with systemic administration of recombinant therapeutic proteins, including insufficient drug penetration, a hostile tumor microenvironment and significant side effects.

The rationale for developing an *in situ* programming reagent, rather than exploring the adoptive transfer of *ex vivo* genetically engineered monocytes/macrophages, is that nanomedicines can be readily fabricated on a large scale and in a stable form, are easy to distribute as lyophilized reagents, are inexpensive to administer, and can be delivered to sizeable patient populations in outpatient settings. Macrophage-based cell-therapy products have entered clinical testing for anticancer activity or tolerance induction [32,33]. However, the elaborate and expensive protocols currently required to manufacture engineered macrophages *ex vivo* put this approach beyond the reach of many patients who might benefit. Harnessing synthetic nanoparticles as reagents for selective *in situ*-reprogramming of monocytes/macrophages for therapeutic purposes comes with notable advantages. For example, macrophages are inherently phagocytic cells that are extremely effective at clearing nanomaterials [34], and they are present in high numbers, thus ensuring high transfection rates with only moderate off-target gene transfer. Moreover, they can quickly and directionally migrate to pathological sites such as tumor lesions or inflamed tissue [35,36]. This native homing ability favors them as vehicles for the focused delivery and expression of therapeutic transgenes at the disease site.

We developed a targeted mRNA – rather than a plasmid DNA – delivery system. Unlike other mammalian cells, macrophages are difficult to transfect with plasmid DNA, not only because they have evolved to recognize foreign nucleic acids and to initiate an immune response to these molecules, but mostly because they are almost non-proliferating cells [37]. Thus, timely arrival at the nucleus during mitotic envelope breakdown is challenging for plasmid DNA.

More than 100 bispecific T-cell engager formats have been described and novel structures of BiTES are emerging constantly [38], not only for the treatment of malignancies but also for a range of autoimmune diseases such as rheumatoid arthritis, systemic lupus erythematosus, and psoriasis [39]. Our approach therefore has the potential to provide the basis for a broad range of clinical applications.

Supplementary Material

Refer to Web version on PubMed Central for supplementary material.

Acknowledgments

This research was supported by the Experimental Histopathology Shared Resource, the Genomics Shared Resource, and the Comparative Medicine Shared Resource of the Fred Hutch/University of Washington Cancer Consortium (P30 CA015704). M.T. Stephan was also supported by the NCI (CA207407, CA261858) and Tidal Therapeutics (a Sanofi Company).

References

- [1]. Goebeler ME, Bargou RG, T cell-engaging therapies - BiTEs and beyond, *Nat. Rev. Clin. Oncol* 17 (2020) 418–434. [PubMed: 32242094]
- [2]. Singh A, Dees S, Grewal IS, Overcoming the challenges associated with CD3+ T-cell redirection in cancer, *Br. J. Cancer* 124 (2021) 1037–1048. [PubMed: 33469153]
- [3]. Bukhari A, Lee ST, Blinatumomab: a novel therapy for the treatment of non-Hodgkin's lymphoma, *Expert. Rev. Hematol* 12 (2019) 909–918. [PubMed: 31583919]
- [4]. Yuraszek T, Kasichayanula S, Benjamin JE, Translation and clinical development of bispecific T-cell engaging antibodies for cancer treatment, *Clin. Pharmacol. Ther* 101 (2017) 634–645. [PubMed: 28182247]
- [5]. Kantarjian H, et al. , Blinatumomab versus chemotherapy for advanced acute lymphoblastic leukemia, *N. Engl. J. Med* 376 (2017) 836–847. [PubMed: 28249141]
- [6]. Ferrari F, et al. , Solitomab, an EpCAM/CD3 bispecific antibody construct (BiTE (R)), is highly active against primary uterine and ovarian carcinosarcoma cell lines in vitro, *J. Exp. Clin. Cancer Res* 34 (2015) 123. [PubMed: 26474755]
- [7]. Richter CE, et al. , High-grade, chemotherapy-resistant ovarian carcinomas overexpress epithelial cell adhesion molecule (EpCAM) and are highly sensitive to immunotherapy with MT201, a fully human monoclonal anti-EpCAM antibody, *Am. J. Obstet. Gynecol* 203 (582) (2010) e581–e587.
- [8]. Schmelzer E, Reid LM, EpCAM expression in normal, non-pathological tissues, *Front. Biosci* 13 (2008) 3096–3100. [PubMed: 17981779]
- [9]. Kebenko M, et al. , A multicenter phase I study of solitomab (MT110, AMG 110), a bispecific EpCAM/CD3 T-cell engager (BiTE(R)) antibody construct, in patients with refractory solid tumors, *Oncoimmunology* 7 (2018), e1450710. [PubMed: 30221040]
- [10]. Haense N, et al. , A phase I trial of the trifunctional anti Her2 x anti CD3 antibody ertumaxomab in patients with advanced solid tumors, *BMC Cancer* 16 (2016) 420. [PubMed: 27387446]
- [11]. Kiewe P, et al. , Phase I trial of the trifunctional anti-HER2 x anti-CD3 antibody ertumaxomab in metastatic breast cancer, *Clin. Cancer Res* 12 (2006) 3085–3091. [PubMed: 16707606]
- [12]. Mau-Sorensen M, et al. , A phase I trial of intravenous catumaxomab: a bispecific monoclonal antibody targeting EpCAM and the T cell coreceptor CD3, *Cancer Chemother. Pharmacol* 75 (2015) 1065–1073. [PubMed: 25814216]
- [13]. Choi BD, et al. , CAR-T cells secreting BiTEs circumvent antigen escape without detectable toxicity, *Nat. Biotechnol* 37 (2019) 1049–1058. [PubMed: 31332324]
- [14]. Heidbuechel JPW, Engeland CE, Oncolytic viruses encoding bispecific T cell engagers: a blueprint for emerging immunovirotherapies, *J. Hematol. Oncol* 14 (2021) 63. [PubMed: 33863363]
- [15]. Lemos de Matos A, Franco LS, McFadden G, Oncolytic viruses and the immune system: the dynamic duo, *Mol. Ther. Methods Clin. Dev* 17 (2020) 349–358. [PubMed: 32071927]
- [16]. Van Hoecke L, Roose K, How mRNA therapeutics are entering the monoclonal antibody field, *J. Transl. Med* 17 (2019) 54. [PubMed: 30795778]
- [17]. Cross R, Can mRNA disrupt the drug industry? *Chem. Eng. News* 96 (2018) 34–40.
- [18]. Jackson NAC, Kester KE, Casimiro D, Gurunathan S, DeRosa F, The promise of mRNA vaccines: a biotech and industrial perspective, *NPJ Vaccin.* 5 (2020) 11.
- [19]. Kariko K, et al. , Incorporation of Pseudouridine into mRNA yields superior nonimmunogenic vector with increased translational capacity and biological stability, *Mol. Ther* 16 (2008) 1833–1840. [PubMed: 18797453]
- [20]. Nallagatla SR, Bevilacqua PC, Nucleoside modifications modulate activation of the protein kinase PKR in an RNA structure-specific manner, *Rna* 14 (2008) 1201–1213. [PubMed: 18426922]
- [21]. Kariko K, Weissman D, Naturally occurring nucleoside modifications suppress the immunostimulatory activity of RNA: implication for therapeutic RNA development, *Curr. Opin. Drug. Disc* 10 (2007) 523–532.

- [22]. Muttach F, Muthmann N, Rentmeister A, Synthetic mRNA capping, *Beilstein J. Org. Chem* 13 (2017) 2819–2832. [PubMed: 30018667]
- [23]. Elliott LA, Doherty GA, Sheahan K, Ryan EJ, Human tumor-infiltrating myeloid cells: phenotypic and functional diversity, *Front. Immunol* 8 (2017) 86. [PubMed: 28220123]
- [24]. Roby KF, et al. . Development of a syngeneic mouse model for events related to ovarian cancer, *Carcinogenesis* 21 (2000) 585–591. [PubMed: 10753190]
- [25]. Quabius ES, Krupp G, Synthetic mRNAs for manipulating cellular phenotypes: an overview, *New Biotechnol.* 32 (2015) 229–235.
- [26]. Liao JB, et al. . Preservation of tumor-host immune interactions with luciferase-tagged imaging in a murine model of ovarian cancer, *J. Immunother. Cancer* 3 (2015) 16. [PubMed: 25992288]
- [27]. Stephan SB, et al. . Biopolymer implants enhance the efficacy of adoptive T-cell therapy, *Nat. Biotechnol* 33 (2015) 97–101. [PubMed: 25503382]
- [28]. Kim SR, et al. . Efficacy and toxicity of intraperitoneal chemotherapy as compared to intravenous chemotherapy in the treatment of patients with advanced ovarian cancer, *Int. J. Gynaecol. Obstet* (2021), 10.1002/ijgo.13813.
- [29]. Miller SI, et al. . Hypoglycemia as a manifestation of Sepsis, *Am. J. Med* 68 (1980) 649–654. [PubMed: 6990758]
- [30]. Khadka RH, Sakemura R, Kenderian SS, Johnson AJ, Management of cytokine release syndrome: an update on emerging antigen-specific T cell engaging immunotherapies, *Immunotherapy-Uk* 11 (2019) 851–857.
- [31]. Kauffman KJ, et al. . Rapid, single-cell analysis and discovery of vectored mRNA transfection in vivo with a loxP-flanked tdTomato reporter mouse, *Mol. Ther. Nucleic Acids* 10 (2018) 55–63. [PubMed: 29499956]
- [32]. Mukhopadhyay M, Macrophages enter CAR immunotherapy, *Nat. Methods* 17 (2020) 561. [PubMed: 32499619]
- [33]. Anderson NR, Minutolo NG, Gill S, Klichinsky M, Macrophage-based approaches for cancer immunotherapy, *Cancer Res.* 81 (2021) 1201–1208. [PubMed: 33203697]
- [34]. Gustafson HH, Holt-Casper D, Grainger DW, Ghandehari H, Nanoparticle uptake: the phagocyte problem, *Nano Today* 10 (2015) 487–510. [PubMed: 26640510]
- [35]. Nourshargh S, Alon R, Leukocyte migration into inflamed tissues, *Immunity* 41 (2014) 694–707. [PubMed: 25517612]
- [36]. Nielsen SR, Schmid MC, Macrophages as key drivers of cancer progression and metastasis, *Mediat. Inflamm* 2017 (2017).
- [37]. Zhang X, Edwards JP, Mosser DM, The expression of exogenous genes in macrophages: obstacles and opportunities, *Methods Mol. Biol* 531 (2009) 123–143. [PubMed: 19347315]
- [38]. Brinkmann U, Kontermann RE, The making of bispecific antibodies, *Mabs-Austin* 9 (2017) 182–212.
- [39]. Zhao Q, Bispecific antibodies for autoimmune and inflammatory diseases: clinical progress to date, *Biodrugs* 34 (2020) 111–119. [PubMed: 31916225]

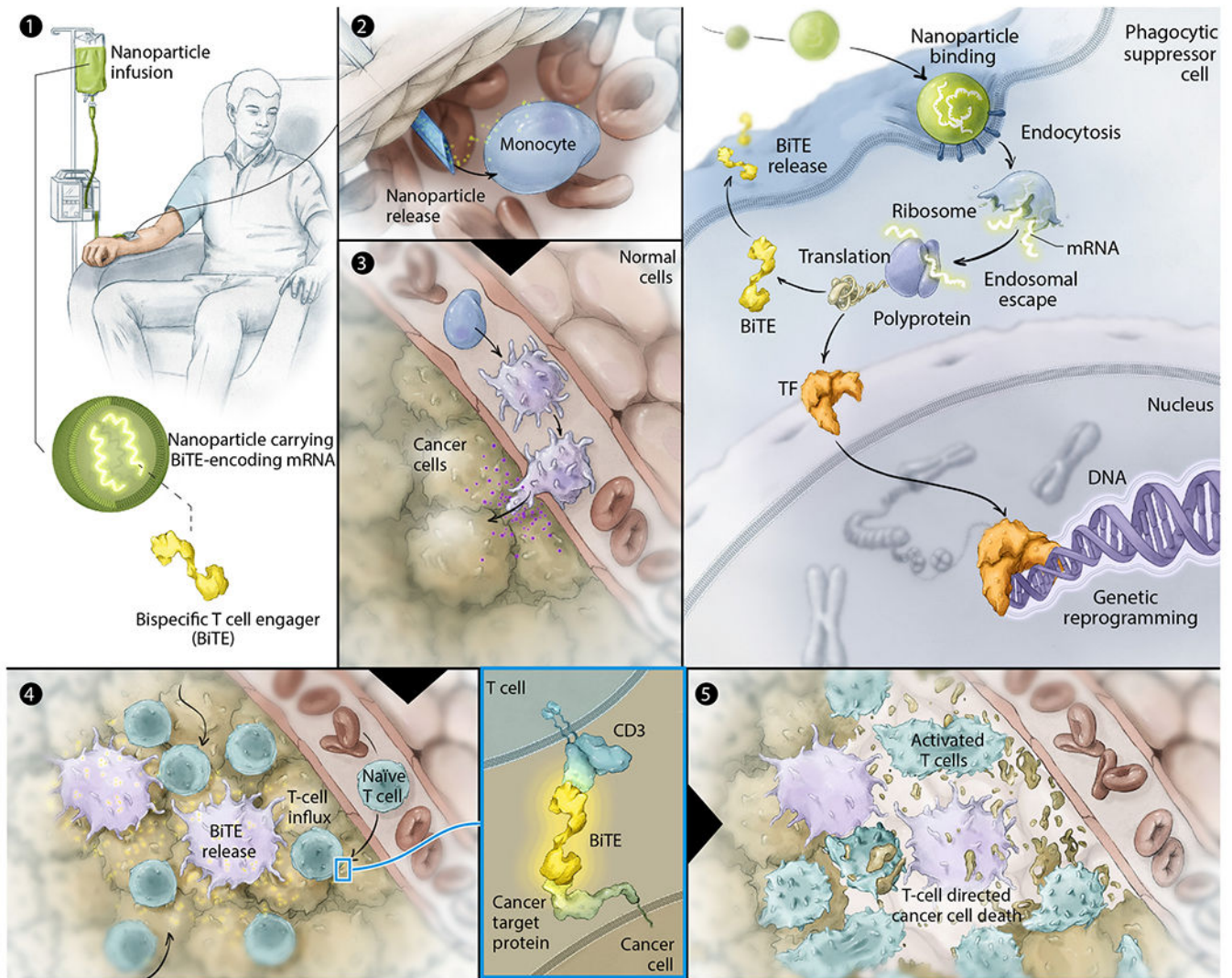


Fig. 1. Schematic illustrating how we reprogram circulating myeloid cells to direct BiTE expression to tumor sites, using targeted nanocarriers.

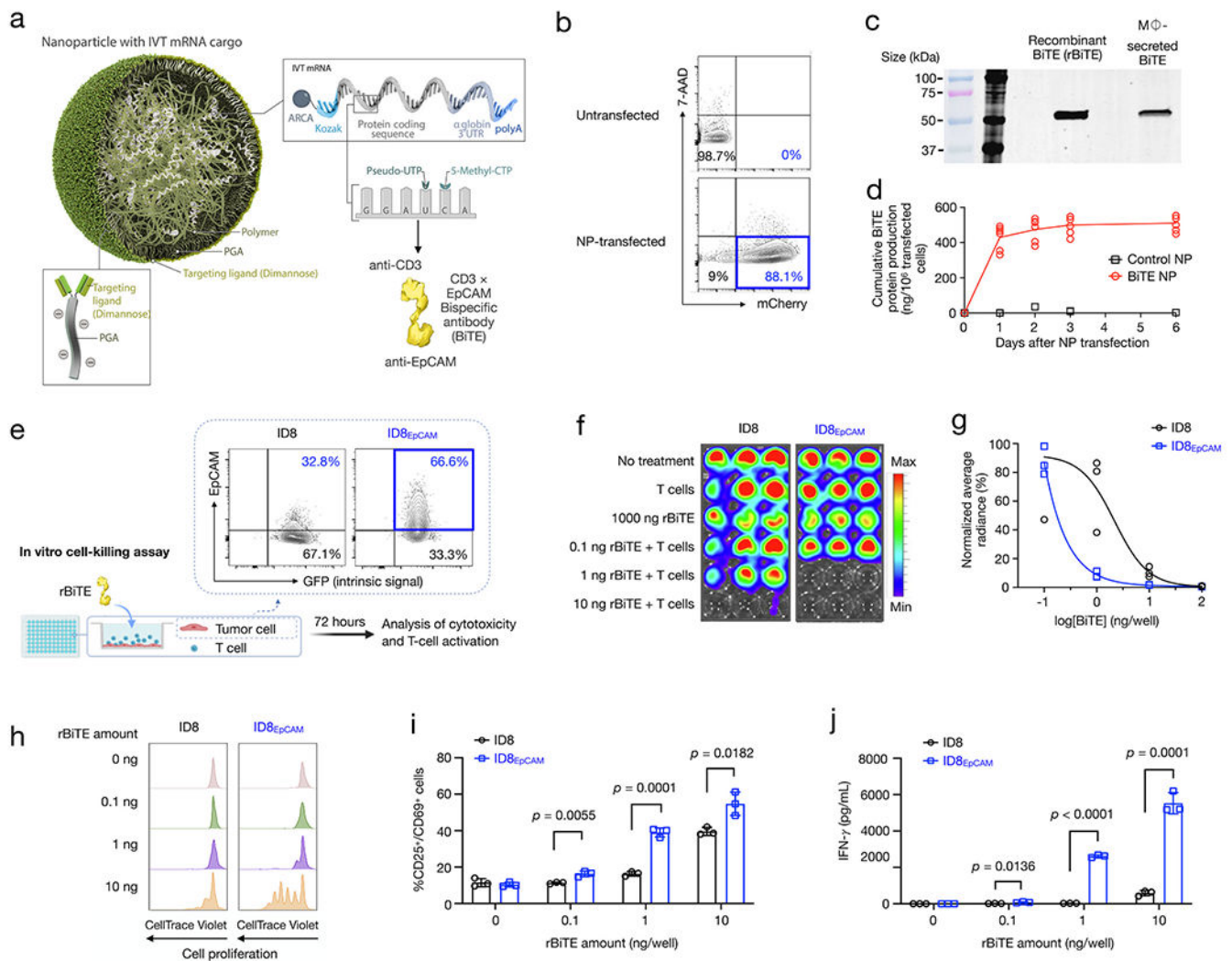


Fig. 2. Macrophage transfection with BiTE-encoding mRNA nanocarriers results in functional BiTE protein secretion. (a) Design of macrophage-targeted polymeric nanoparticles formulated with mRNAs encoding the CD3 × EpCAM bispecific antibody. The particles consist of a PbAE-mRNA polyplex core coated with a layer of PGA-Di-mannose, which targets the particles to mannose receptors (CD206). Also depicted is the synthetic mRNA encapsulated in the nanoparticles, which is engineered to encode the bispecific antibody. (b) Flow cytometric analysis of gene-transfer efficiencies into RAW 264.7 macrophages. (c) Immunoblot detection with an IRDye 680RD Streptavidin-conjugated antibody to C-tagged CD3 × EpCAM bispecific antibody in supernatants from nanoparticle-transfected RAW 264.7 macrophages. Positive control, 25 ng of the corresponding purified recombinant BiTE protein. (d) ELISA measurements of EpCAM × CD3 BiTE protein production by nanoparticle-transfected (mCherry⁺) RAW264.7 cells. Assays were performed in triplicate. (e-j) Assessing T-cell activation, cytokine secretion and cytotoxicity against tumor cells. (e) Schematic representation of *in vitro* cell-killing assays conducted by adding escalating doses of rBiTE into co-cultures of tumor cells and naive T cells. ID8_{EpCAM} cells are

lentivirally engineered versions of ID8 ovarian tumor cells that stably express EpCAM. Tumor lysis and T-cell activation were evaluated by bioluminescent imaging and flow cytometry, respectively, after 72 h of incubation. (f) Bioluminescence imaging of ID8 cells or ID8_{EpCAM} cells cultured in 96-well plates under different conditions. (g) Levels of bioluminescent signals in (f) were summarized as normalized average radiances in a dose-response curve. (h) Representative flow cytometric histograms demonstrating T-cell proliferation after 72 h of co-culturing with tumor cells in the presence of different amounts of rBiTE. (i) Flow cytometric quantitation of activated T cells. (j) Cytokine secretion was determined by Luminex assay. Assays were performed in triplicate. Means \pm SD are depicted. NP, nanoparticle; rBiTE, recombinant BiTE protein.

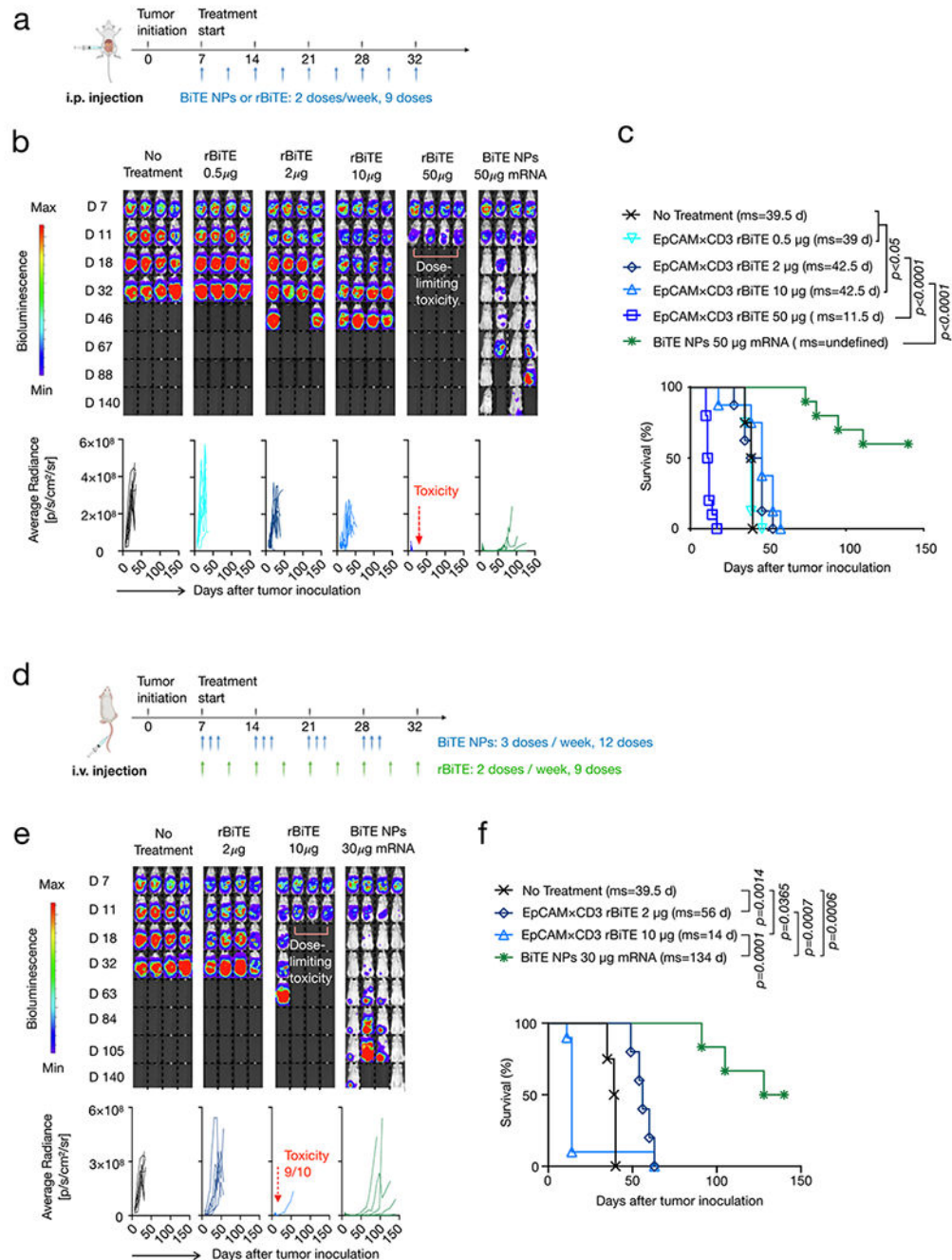


Fig. 3. BiTE mRNA nanoparticles improve the narrow therapeutic window of EpCAM \times CD3 BiTE recombinant protein and extend the survival of mice with ovarian cancer. (a) Timelines and dosing regimens for intraperitoneal (i.p.)-delivered rBiTE and BiTE nanoparticles. Escalating doses of rBiTE (0.5 μg , 2 μg , 10 μg , and 50 μg) and BiTE nanoparticles containing 50 μg mRNA were injected i.p. into mice with ovarian cancer at 2 doses per week for a total of 9 doses. Treatment started at 7 days after tumor inoculation. (b) Representative sequential bioluminescence imaging of tumor growth and the quantified tumor burden over

time (as radiance from luciferase activity from each mouse). (c) Kaplan-Meier survival curves. Statistical analysis was performed using the log-rank test. $N= 8$ biologically independent animals. (d) Timelines and dosing regimens for intravenously (i.v.)-delivered rBiTE and BiTE nanoparticles. (e) Representative sequential bioluminescence imaging of tumor growth and the quantified tumor burden over time (as radiance from luciferase activity from each mouse). (f) Kaplan-Meier survival curves. Statistical analysis was performed using the log-rank test.

Author Manuscript

Author Manuscript

Author Manuscript

Author Manuscript

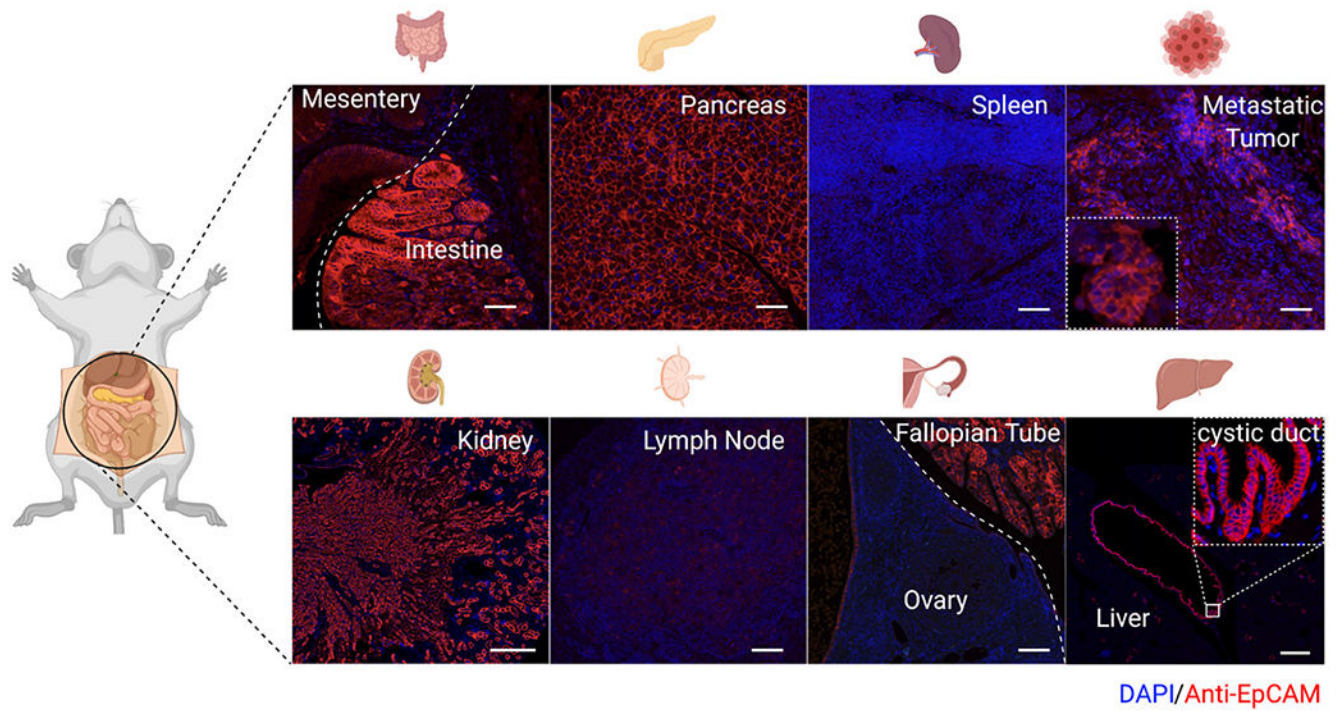


Fig. 4. EpCAM is expressed in non-pathological tissue as well as malignant lesions. Confocal microscopy of various healthy tissues isolated from C57BL/6 mice and ID8-VEGF-EpCAM ovarian tumor lesions. The expression of EpCAM was assessed by immunofluorescence, and representative staining results for each tissue are shown. Scale bars, liver and kidney: 500 μm; all other organs: 50 μm.

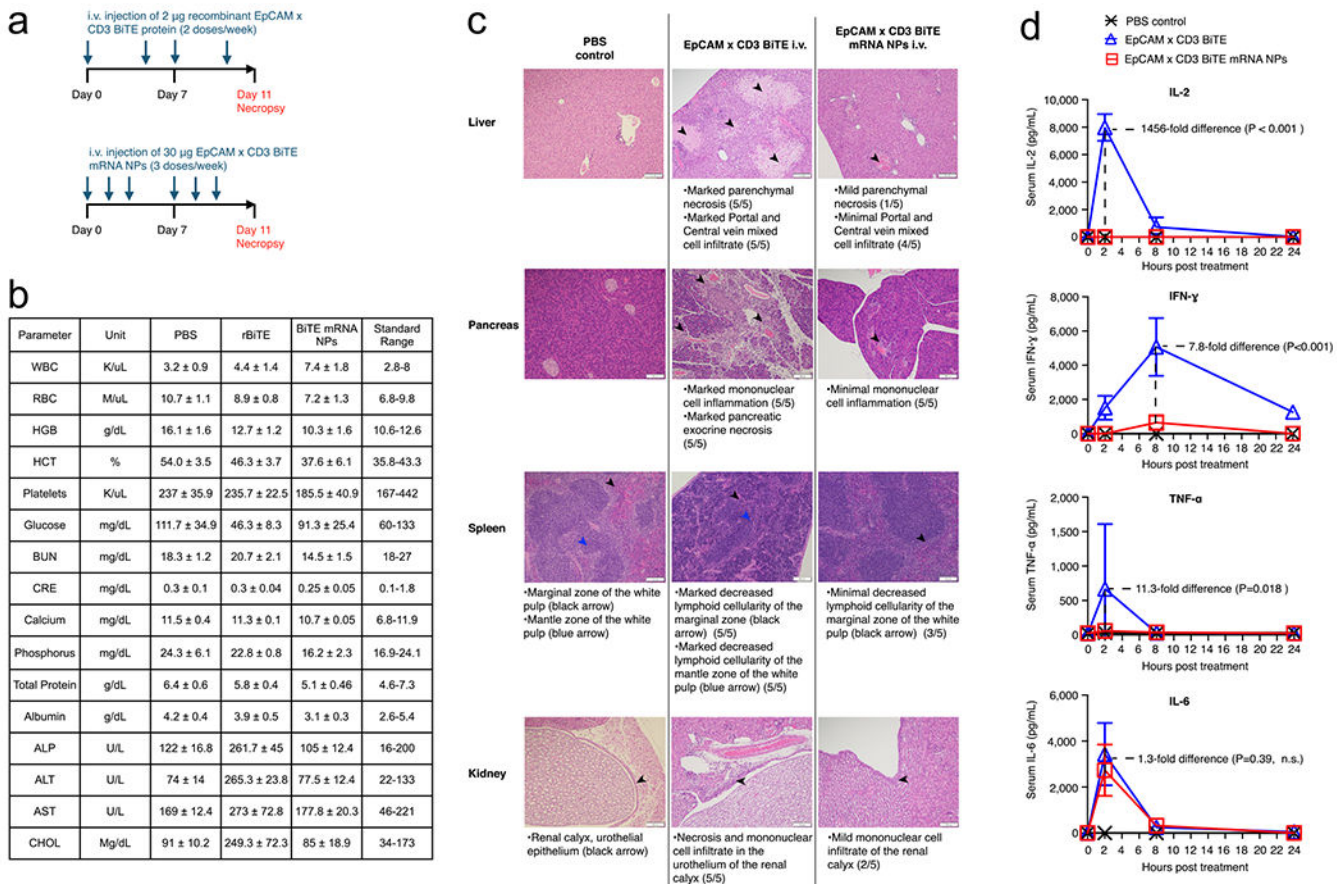


Fig. 5. Secretion of T-cell engagers from *in situ*-programmed myeloid cells overcomes autoimmune toxicities of conventional injections of recombinant BiTE protein. (a) Schematic representation of the experimental timeline. (b) Serum chemistry and blood counts. (c) Representative H&E-stained sections of various organs isolated from PBS controls, recombinant BiTE- or nanoparticle-treated animals. Scale bars, 100 µm. Lesions found in the animals are shown and they are described beneath each image. (d) Serial Luminex assay measurements of serum IL-2, IFN- γ , TNF- α and IL-6 cytokines.

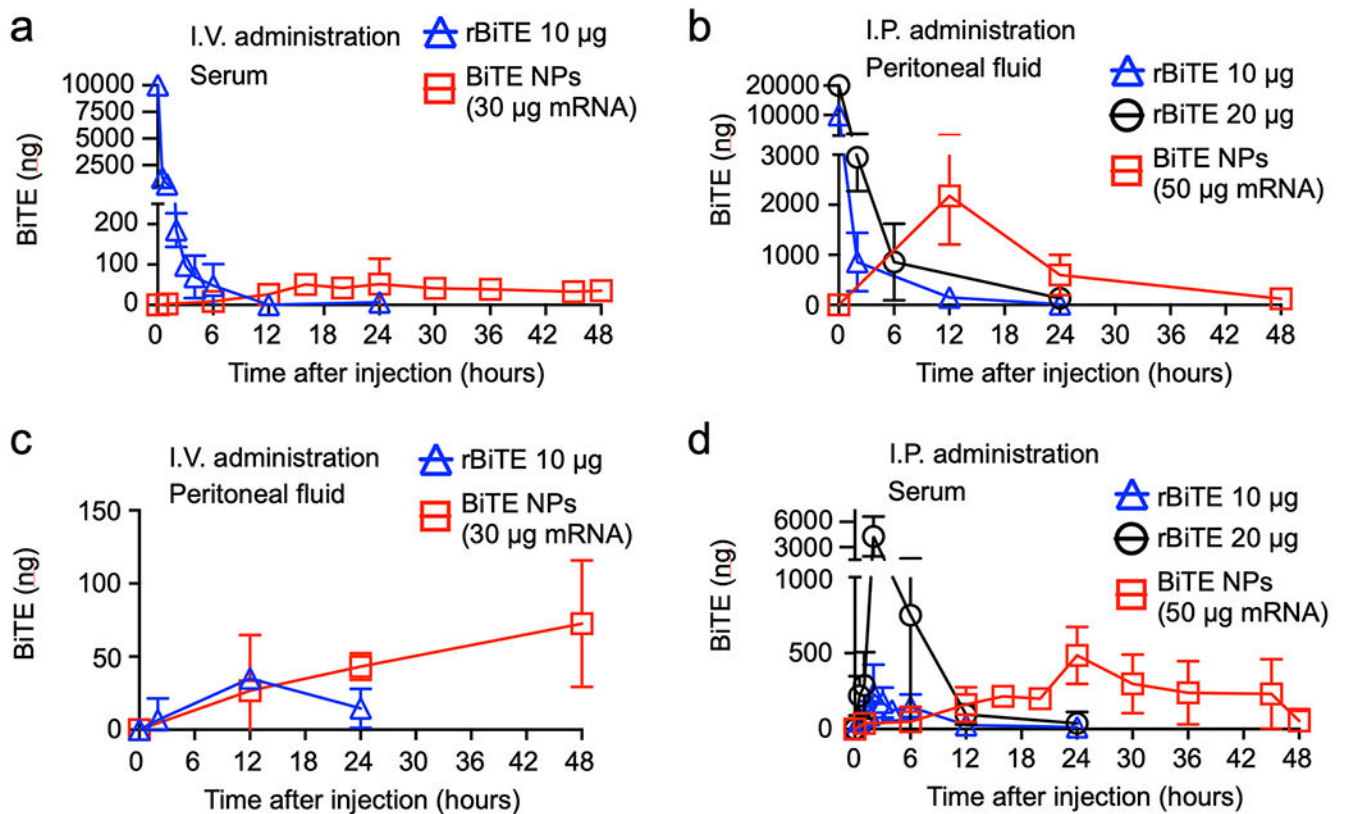


Fig. 6. Limited systemic drug exposure following secretion of BiTE antibodies by nanoparticle-transfected macrophages. Quantitative analysis of EpCAM \times CD3 BiTE protein in the serum or peritoneal fluid of mice with established ID8-VEGF-EpCAM ovarian tumor lesions. Mice received a single-bolus injection of recombinant BiTE protein (rBiTE) or BiTE-encoding mRNA nanoparticles (BiTE NPs) administered intravenously or intraperitoneally. At the indicated time points, EpCAM \times CD3 BiTE protein amounts were quantified by c-tag ELISA. $N = 9$ biologically independent samples. Shown are mean values \pm SD.

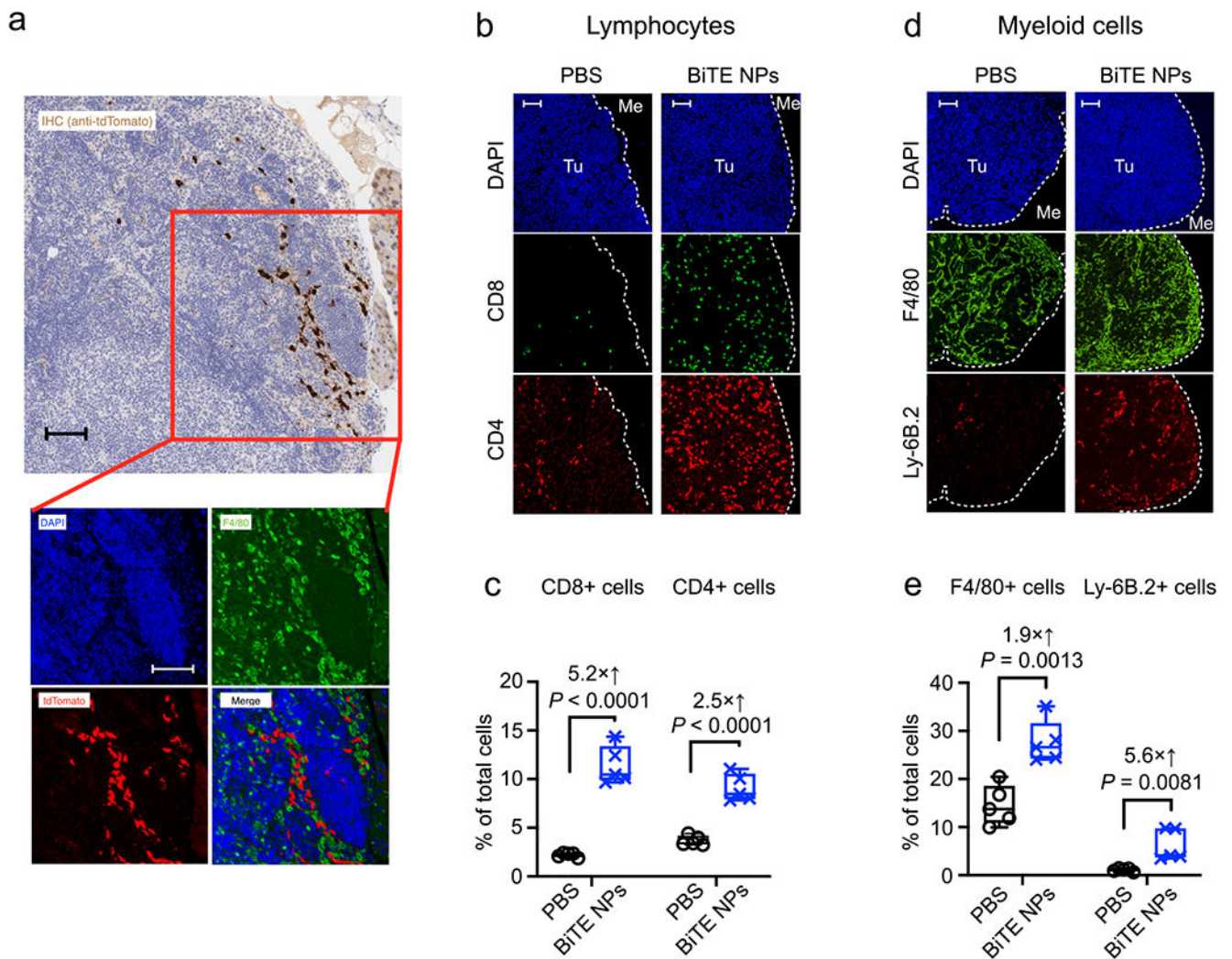


Fig. 7. BiTE nanoparticle-transfected macrophages infiltrate solid tumors and recruit cytotoxic T cells. (a) Immunohistochemical (IHC) staining (top panel) and immunofluorescence staining (bottom panel) of ID8-VEGF-EpCAM ovarian tumors isolated from Ai14 reporter mice treated with PBS or Cre mRNA nanoparticles (3 weekly 50 μ g mRNA doses for 2 weeks). Tissues were stained for the indicated markers. Tu = Tumor, Me = Mesentery. Scale bars: 100 μ m. (b, d) Representative confocal images of peritoneal metastases of ID8-VEGF-EpCAM ovarian cancer cells in the mesentery. Tissues were collected after 6 twice-weekly i.p. injections of PBS or EpCAM \times CD3 BiTE mRNA nanoparticles (50 μ g mRNA/dose), and were stained for the indicated lymphocyte- and myeloid-markers (Tu = Tumor, Me = Mesentery). Scale bars: 100 μ m). (c, e) Bar graphs showing fluorescent signals for each phenotypic marker using HaloTM image analysis software. $N = 5$.

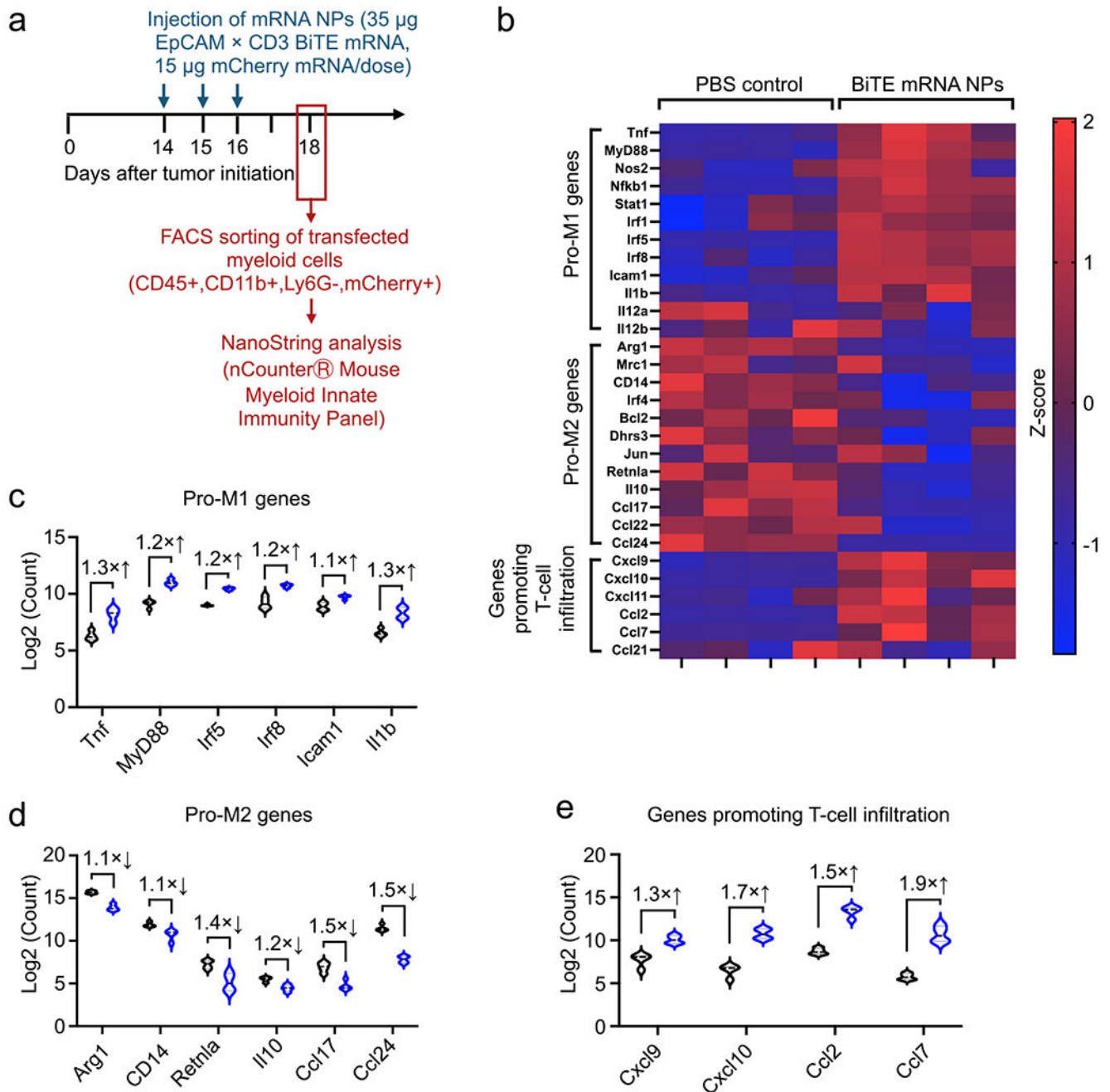


Fig. 8. BiTE-encoding nanoparticles can imprint a pro-inflammatory M1-like phenotype. (a) Experimental timeline of the gene expression study. (b) Heat map of signature gene expression in nanoparticle-transfected (mCherry+) myeloid cells sorted from ovarian tumor-bearing mice following EpCAM \times CD3 BiTE mRNA nanoparticle therapy or PBS control treatment. Abundances of mRNAs were normalized by z-scores created with the equation $z = (x - \bar{x}) / SD(x)$. (c-e) Violin plots showing counts for the indicated genes. $N = 6$ biologically independent samples.